

ANESTHESIOLOGY

Inhibition of Sphingosine Kinase 1 Attenuates Sepsis-induced Microvascular Leakage via Inhibiting Macrophage NLRP3 Inflammasome Activation in Mice

Ming Zhong, M.D., Ph.D., Wei Wu, M.D.,
Yingqin Wang, M.S., Hailei Mao, M.D.,
Jieqiong Song, M.D., Song Chen, M.D., Duming Zhu, M.D.

ANESTHESIOLOGY 2020; 132:1503–15

EDITOR'S PERSPECTIVE

What We Already Know about This Topic

- Nucleotide-binding oligomerization domain-like receptor containing pyrin domain 3 (NLRP3) inflammasomes are intracellular multiprotein complexes in innate immune cells that may be activated in sepsis
- Sphingosine-1-phosphate is a bio lipid that has been suggested to be involved in NLRP3 activation, but its role in sepsis and NLRP3 inflammasome activation is not understood
- Sphingosine kinase 1 mediates sphingosine-1-phosphate formation

What This Article Tells Us That Is New

- In peripheral blood mononuclear cells from septic patients, lipopolysaccharide-stimulated sphingosine-1-phosphate messenger RNA expression was higher than in cells from healthy volunteers
- In male mouse model of sepsis, treatment with a specific inhibitor of sphingosine kinase 1 decreased mortality, improved peripheral perfusion, and diminished capillary leak
- Results suggest that sphingosine kinase 1 may participate in NLRP3 activation, and septic lung injury and mortality in mice

Sepsis, defined as a dysregulated host immune response to infection, is a leading cause of hospital mortality.¹ Despite enormous progress in supportive care, outcomes

ABSTRACT

Background: Sepsis is the overwhelming inflammatory response to infection, in which nucleotide-binding oligomerization domain-like receptor containing pyrin domain 3 (NLRP3) inflammasome plays a crucial role. Sphingosine-1-phosphate is reported to evoke NLRP3 inflammasome activation. Sphingosine kinase 1 (SphK1) is the major kinase that catalyzes bioactive lipid sphingosine-1-phosphate formation and its role in sepsis remains uncertain. The authors hypothesize that SphK1 elicits NLRP3 inflammasome activation and exacerbates sepsis.

Methods: Peripheral blood mononuclear cells were isolated from septic patients and healthy volunteers to measure messenger RNA (mRNA) expression. In mice, sepsis was induced by cecal ligation and puncture. Bone marrow-derived macrophages were prepared from C57BL/6J wild-type, *Casp1*^{−/−}, *Nlrp3*^{−/−} and *SphK1*^{−/−} mice. PF-543 was used as the specific inhibitor of SphK1. Mortality, peripheral perfusion, lung Evan's blue dye index, lung wet/dry ratio, lung injury score, lung myeloperoxidase activity, NLRP3 activation, and function of endothelial adherens junction were measured.

Results: *SphK1* mRNA expression was higher in cells from septic patients versus healthy volunteers (septic patients vs. healthy volunteers: 50.9 ± 57.0 fold change vs. 1.2 ± 0.1 fold change, $P < 0.0001$) and was positively correlated with *IL-1β* mRNA expression in these cells ($r = 0.537$, $P = 0.012$) and negatively correlated with $\text{PaO}_2/\text{FiO}_2$ ratios ($r = 0.516$, $P = 0.017$). In mice that had undergone cecal ligation and puncture, the 5-day mortality was 30% in PF-543-treated group and 80% in control group ($n = 10$ per group, $P = 0.028$). Compared with controls, PF-543-treated mice demonstrated improved peripheral perfusion and alleviated extravascular Evan's blue dye effusion (control vs. PF-543: 25.5 ± 3.2 ng/g vs. 18.2 ± 1.4 ng/g, $P < 0.001$), lower lung wet/dry ratio (control vs. PF-543: 8.0 ± 0.2 vs. 7.1 ± 0.4, $P < 0.0001$), descending lung injury score, and weaker lung myeloperoxidase activity. Inhibition of SphK1 suppressed caspase-1 maturation and interleukin-1β release through repressing NLRP3 inflammasome activation, and subsequently stabilized vascular endothelial cadherin through suppressing interleukin-1β-evoked Src-mediated phosphorylation of vascular endothelial cadherin.

Conclusions: SphK1 plays a crucial role in NLRP3 inflammasome activation and contributes to lung injury and mortality in mice polymicrobial sepsis.

(ANESTHESIOLOGY 2020; 132:1503–15)

of severe septic patients remain unsatisfied. Early mortality of sepsis is predominantly attributed to excessive inflammatory response to pathogens, which leads to subsequent hemodynamic collapse and multiple organ dysfunction.² Therefore, targeting overwhelming inflammation in the initiation of sepsis is of considerable interest for developing new treatment options.

Nucleotide-binding oligomerization domain-like receptor containing pyrin domain 3 (NLRP3) inflammasomes are

Supplemental Digital Content is available for this article. Direct URL citations appear in the printed text and are available in both the HTML and PDF versions of this article. Links to the digital files are provided in the HTML text of this article on the Journal's Web site (www.anesthesiology.org). M.Z. and W.W. contributed equally to this article.

Submitted for publication November 20, 2018. Accepted for publication January 2, 2020. Published online first on February 27, 2020. From the Department of Critical Care Medicine, Zhongshan Hospital, Fudan University, Shanghai, China.

Copyright © 2020, the American Society of Anesthesiologists, Inc. All Rights Reserved. Anesthesiology 2020; 132:1503–15. DOI: 10.1097/ALN.0000000000003192

intracellular multiprotein complexes in innate immune cells that play a key role in triggering inflammatory responses after infection.³ The multiprotein complex comprises the sensor molecule NLRP3, the adaptor protein apoptosis-associated speck-like protein containing a caspase recruitment domain (ASC), and pro-caspase-1. On sensing exogenous pathogens or endogenous danger signals, NLRP3 recruits ASC and pro-caspase-1, leading to caspase-1 activation, and maturation and release of proinflammatory cytokines interleukin-1 β and interleukin-18.⁴ NLRP3 inflammasomes in macrophages participate in the pathogenesis of various diseases characterized by unrestrained inflammatory activation, such as acute lung injury and sepsis.^{5–8} It is reported that the *Nlrp3* deficient mice are more resistant to sepsis than wild-type mice.^{8,9} Functionally, *Nlrp3* deficiency protects mice from excessive proinflammatory cytokine storm, vascular leakage, and tissue damage in cecal ligation and puncture-induced sepsis.⁸ In addition, evidence shows that inhibition of NLRP3 may also contribute to resolution of inflammation.⁸ Nevertheless, the underlying mechanism for NLRP3 inflammasome activation in sepsis remains elusive.

Sphingosine-1-phosphate, generated from sphingosine by two isoforms of sphingosine kinases (SphK1 and SphK2), is a bioactive lipid that regulates diverse biologic processes. The proinflammatory roles of sphingosine-1-phosphate have been emphasized in inflammatory diseases, including ulcerative colitis, asthma, and autoimmune disorders.^{10–13} SphK1 is the major kinase that generates sphingosine-1-phosphate in blood,¹⁴ and its protein expression and enzymatic activity are both upregulated in macrophages during endotoxemia.^{15–17} Recently, sphingosine-1-phosphate has been suggested to be involved in NLRP3 activation.¹⁸ However, the roles of SphK1 in polymicrobial sepsis and NLRP3 inflammasome activation have not been well addressed. We hypothesize that SphK1 promotes macrophage NLRP3 inflammasome activation and exacerbates inflammation in polymicrobial sepsis. Therefore, we used a novel selective SphK1 inhibitor, PF-543, to investigate the roles of SphK1 in sepsis and NLRP3 inflammasome activation.

Materials and Methods

Human Studies

Human Subjects. Adult patients diagnosed with sepsis in Surgical Intensive Care Unit (Zhongshan Hospital, Fudan University, Shanghai, China) between March 2014 to April 2019 were eligible for inclusion. Nonseptic patients who were admitted in the same time period after elective surgery were recruited with similar age and sex ratio. Adult healthy volunteers were also recruited with similar age and sex ratio. All patients were recruited in the study under informed consent guidelines approved by the Ethics Committee of Zhongshan Hospital, Fudan University (B2017-021R). Written informed consent was obtained from patients or their statutory surrogates. Patients' characteristics such as sex, Sequential Organ Failure Assessment score, primary

site of infection, and diagnosis were recorded at admission. Peripheral blood was sampled from patients within the first 24 h after admission. PaO₂/Fio₂ ratio was recorded at time point of sample collection. Correlation of interleukin-1 β messenger RNA (mRNA) expression in peripheral blood mononuclear cells and PaO₂/Fio₂ ratios with SphKs mRNA expression were examined with Pearson correlation coefficient, and then linear regression analysis with a 95% confidence interval was performed.

Quantitative Real-time Polymerase Chain Reaction. Ficoll-Hypaque (GE Healthcare, USA) was used to separate peripheral blood mononuclear cells from blood samples of septic patients, nonseptic patients, and healthy volunteers according to manufacturer's instructions. The total RNA was extracted using TRIzol reagent (Invitrogen, USA). The RNA isolated from peripheral blood mononuclear cells was converted to cDNA using the Reverse Transcription Master Mix (EZBioscience, USA). Quantitative real-time polymerase chain reaction was performed using SYBR Green qPCR Master Mix (EZBioscience) according to manufacturer's protocols. Primers are listed in table S1 (Supplemental Digital Content, <http://links.lww.com/ALN/C272>). Results were analyzed using the comparative cycle-threshold method, where the amount of target gene was normalized to an endogenous reference gene, GAPDH.

Micro-array Gene Expression Analysis. The mRNA expressions of *SphK1* and *SphK2* in healthy human adult peripheral blood mononuclear cells (monocytes) were obtained from Gene Expression Omnibus.¹⁹ The original dataset was downloaded (GSE3140). *SphK1* gene was validated as 219257_s_at, and *SphK2* gene was validated as 40273_at. The differentially expressed mRNA expressions of *SphK1* and *SphK2* were analyzed in healthy human monocytes treated with lipopolysaccharide (100 ng/ml, 4h).

Animal Studies

Animals. Experiments were performed under protocols approved by the Animal Care and Use Committee of the Zhongshan Hospital, Fudan University. Eight-to-twelve-week old, 20- to 25-g, male C57BL/6J wild-type, *Casp1*^{-/-}, *Nlrp3*^{-/-}, and *SphK1*^{-/-} mice (Cyagen Biosciences, USA) were used in the experiments. All mice were bred and housed in a specific pathogen-free facility with soft bedding and were given food and water *ad libitum*, with a 12:12 light:dark cycle.

Surgery and Drugs. Each mouse was assigned a random number that was generated by Microsoft Excel 2016 (USA). The assigned numbers were sorted from the smallest to the largest, and then the mice were allocated to different experimental groups. All *in vivo* experiments and data collection were conducted with researchers blinded to group assignments. Polymicrobial sepsis was induced by cecal ligation and puncture. Briefly, mice were anesthetized with a mixture of ketamine (80 to 100 mg/kg) and xylazine (10 to 12.5 mg/kg) intraperitoneally. Under aseptic condition,

laparotomy was performed at site of 0.5 cm left to midline of abdomen. After exposure, the cecum was tightly ligated with a 6.0 silk suture (6-0 PROLENE, Ethicon) at the point of 0.5 cm from the distal end of cecum and was perforated twice with a 16-gauge needle. A small amount of feces was gently squeezed out of cecum through perforation sites and the cecum was returned to peritoneal cavity. The same operations were conducted in the sham surgery including opening the peritoneum and exteriorization of cecum. Sham surgery was performed as surgical control. Sterile water was used as solvent of PF-543 and thus used as a drug control in experiments. After surgery, PF-543 (10 mg/kg) or control was injected intraperitoneally. Buprenorphine was used as analgesic. No fluid resuscitation or antibiotics were given. The mice were free to access food and water after surgery. An overdose of isoflurane was used for euthanasia of mice. No animals were excluded after enrollment into the experimental cohorts.

Peripheral Microvascular Perfusion. Twenty-four hours after surgery, mice were placed on light-absorbing pad with an electric heating blanket set for 37°C. Laser Doppler scan (PeriScan PIM3, Somnotec, Singapore) was performed to measure peripheral microvascular blood perfusion according to manufacturer's instructions.

Microvascular Leakage. Evan's blue dye was dissolved in phosphate buffer saline to make 1% solution. Bovine serum albumin was added to a final concentration of 4% (40 mg/ml). Twenty-four hours after surgery, Evan's blue dye conjugated with albumin was retro-orbitally injected into veins at a dose of 8 µl/g body weight. Lungs were perfused with phosphate buffer saline and harvested 30 min later, followed by homogenization with 1 ml phosphate buffer saline. Homogenates were incubated with 2 ml formamide overnight at 60°C. Supernatant was taken for quantification by spectrophotometric method at absorbance of 620 nm. Concentration of Evan's blue dye was normalized to body weight to calculate Evan's blue dye index and expressed as ng/g of body weight.

Assessment of Lung Injury. Twenty-four hours after surgery, lung tissues were harvested from mice. The wet weight was immediately measured. The lung tissues were then dried in an oven at 60°C for 48 h and then the dry weight was measured. Dividing the wet weight by the dry weight was done to calculate the wet/dry ratio. Paraffin-embedded lung tissue sections were stained with hematoxylin and eosin for histology. Lungs were weighed after perfusion with phosphate buffer saline to remove all blood and stored at -80°C before myeloperoxidase assay. Myeloperoxidase activity was assessed as previously described.²⁰ Lung injury scores in mice defined by the American Thoracic Society were calculated.²¹ Briefly, five random fields of five dimensions of histology features were evaluated: (1) neutrophils in the alveolar space, (2) neutrophils in the interstitial space, (3) hyaline membranes, (4) proteinaceous debris filling the airspaces, and (5) alveolar septal thickening. Each of five

histologic findings was graded using a three-tiered schema. If neutrophils in the alveolar airspaces were not visible, a score of zero was recorded. One to five neutrophils gave a score of 1, and more than five neutrophils gave a score of 2. The presence of neutrophils in the interstitium was considered in an analogous manner to neutrophils in the alveolar airspaces. The presence of a single well-formed eosinophilic band of fibrin within the airspace earned a score of 1, whereas multiple hyaline membranes visible in the field were scored as 2. Otherwise, a score of 0 was recorded. Pink proteinaceous debris filling the airspace was considered in an analogous manner to hyaline membranes. Alveolar septal thickening that was less than twice normal, that was twice to four times normal, or that was greater than four times normal earned a score of 0, 1, or 2, respectively. Lung injury score was generated according to the formula: lung injury score = $(20 \times a) + (14 \times b) + (7 \times c) + (7 \times d) + (2 \times e) / (\text{number of fields} \times 100)$.

Cell Culture. Bone marrow-depleted macrophages were prepared from wild-type mice, *Casp1*^{-/-} mice, *Nlrp3*^{-/-} mice, and *SphK1*^{-/-} mice, respectively, and cultured as previously described.²² Macrophages were primed with 1 µg/ml lipopolysaccharide for 3 h, in combination with PF-543 or control, after 3-h starvation. After priming, macrophages were stimulated with 5 mM adenosine triphosphate for 30 min. Cells were lysed for Western blot. Interleukin-1β release in the supernatant was measured by enzyme-linked immunosorbent assay (R&D, USA). Human lung microvascular endothelial cells were cultured in T75 with endothelial cell growth medium-2 (Lonza, USA) supplemented with growth factor and 10% heat-inactivate fetal bovine serum (Invitrogen). Adherent endothelial cells were cultured in eight-well plates and incubated with or without 10 ng/ml recombinant human interleukin-1β for 24 h after overnight starvation. The integrity of endothelial cell monolayers was quantified by transendothelial electrical resistance assay.

Western Blot. Homogenized lung tissues or cells were lysed with radioimmunoprecipitation assay lysis buffer containing protease inhibitor. Protein concentration was measured with Pierce BCA Protein Assay Kit (Thermo Fisher, USA). Cell lysates were boiled followed by gel electrophoresis and transferring onto polyvinylidene difluoride membranes (Bio-Rad, USA). Membranes were blocked with 5% nonfat dry milk in tris-buffered saline with 0.1% Tween 20 for 1 h at room temperature and incubated with primary antibodies overnight at 4°C. Then the membranes were incubated with secondary antibodies for 1 h at room temperature after washing three times. Blots were measured with an enhanced chemical luminescence kit (Thermo Fisher, USA) and quantified with ImageJ software (NIH, USA). Primary antibodies are listed in table S2.

Coimmunoprecipitation. Macrophages were washed in Hank's balanced salt solution with Ca²⁺ and Mg²⁺ briefly, and were lysed in lysis buffer with protease inhibitors. Lysates were kept on ice for 30 min, pipetting up and down

every 10 min before centrifugation at 16,000g for 15 min. For immunoprecipitation, cell lysates were incubated with anti-NLPR3 antibody and rotated end-over-end overnight at 4°C. Then, protein A/G-conjugated agarose beads were added to each sample, and rotated end-over-end for 2 h before centrifugation at 2,500g for 2 min. Supernatant was discarded and beads were washed three times in wash buffer. Protein was eluted from agarose beads by heating in 2× Laemmli buffer with 2-mercaptoethanol for 10 min at 95°C. Blots were probed with anti-caspase-1 and anti-ASC antibodies.

Surface Protein and Intracellular Protein Separation. For vascular endothelial cadherin internalization experiments, cell surface protein was prepared with The Pierce Cell Surface Protein Isolation Kit (Thermo Fisher) as described previously.²³ Briefly, endothelial cells were grown on 10-cm gelatin-coated plates to confluency. One 10-cm plate of cells was used per condition, with conditions being control or 200 ng/ml recombinant human interleukin-1β treatment for 24 h. Next, cells were washed quickly before adding the EZ-Link Sulfo-NHS-SS-Biotin, prepared in Hank's balanced salt solution. Cells were lysed in lysis buffer and sonicated briefly. Lysates were incubated on ice for 30 min. Then, cell lysates were added to each column prepared with NeutrAvidin Agarose slurry and placed in an end-over-end rotator for 1 h. The first flow through fraction was collected as the intracellular fraction, and then the column was washed 3 times. Then, 2× Laemmli buffer with dithiothreitol was added to the columns, which were rotated for 1 h at room temperature to elute the biotinylated proteins as surface fraction. Separated cell fractions were then analyzed by western blot.

Immunofluorescence Microscopy. For preparation of frozen lung tissues, optimum cutting temperature compounds were gently injected through trachea to maintain fluid in lungs. Frozen sections were cut at 5 μm in a cryostat microtome, mounted on microscope slides. Slides were fixed with 4% paraformaldehyde and permeabilized with 0.1% Triton X-100. Slides were probed with primary antibodies of interleukin-1β and vascular endothelial cadherin, and fluorescence-conjugated secondary antibodies. Images were obtained under a Zeiss fluorescence microscope at ×40 magnification.

Statistical Analysis. Statistical power calculation was not conducted before the study, and the sample size was based on our previous experience with this design. A two-tailed independent unpaired Student's *t* test was used to compare two groups. For comparing three or more groups, between-subject one-way ANOVA followed by the Tukey's multiple comparisons *post hoc* test was used. The normality of datasets was tested with Shapiro-Wilk *W* test. To test for homogeneity of variances, the Brown-Forsythe test and an *F* test were used for the ANOVA and unpaired Student's *t* test, respectively. When assumptions of normal distribution or homogeneity of variances were not met, the

nonparametric Mann-Whitney *U* test or unpaired *t* test with Welch's correction was performed instead, respectively. The Kaplan-Meier plot with log-rank (Mantel-Cox) test was used for assessment of survival difference with right censoring. There were no missing data, and outliers were not excluded from the statistical analyzes. A two-tailed hypothesis test was used, and a *P* < 0.05 was considered as statistically significant. The normality of datasets was examined in Stata, version 13.0 (Stata Corporation, USA). Data analyzes were performed in GraphPad Prism 6.01 (GraphPad Software Inc., USA).

Results

SphK1 mRNA Expression in Peripheral Blood Mononuclear Cells Correlates with Interleukin-1β mRNA Expression and PaO₂/Fio₂ Ratios in Septic Patients

We first measured *SphK1* and *SphK2* mRNA expression in peripheral blood mononuclear cells isolated from septic patients and healthy volunteers. Compared with healthy controls, *SphK1* and *SphK2* mRNA expression were higher in the cells from septic patients (50.9 ± 57.0 fold change in septic patients *vs.* 1.2 ± 0.1 fold change in healthy controls, *P* < 0.0001; and 41.4 ± 62.6 fold change in septic patients *vs.* 0.9 ± 0.2 fold change in healthy controls, *P* = 0.021, fig. 1A). Results from Gene Expression Omnibus microarray gene expression analysis indicated that lipopolysaccharide stimulated *SphK1* mRNA expression (7.3 ± 0.3 transformed count in lipopolysaccharide-stimulated group *vs.* 6.4 ± 0.4 transformed count in control group, *P* = 0.038), but not *SphK2* mRNA expression (3.3 ± 0.2 transformed count in lipopolysaccharide-stimulated group *vs.* 3.5 ± 0.2 transformed count in control group, *P* = 0.278) in monocytes of healthy humans (fig. 1B). To further confirm the mRNA profiles of *SphKs* in sepsis, we compared *SphK1* and *SphK2* mRNA expression in peripheral blood mononuclear cells of septic patients with that of non-septic patients. Only *SphK1* mRNA expression in the cells was higher in septic patients compared with non-septic patients (2.6 ± 1.1 fold change in septic patients *vs.* 0.9 ± 0.6 fold change in non-septic patients, *P* = 0.034; Supplemental Digital Content, fig. S1, <http://links.lww.com/ALN/C272>). Interleukin-1β is one of the most important cytokines that trigger cytokine storm in sepsis. Intriguingly, *SphK1* mRNA expression was positively associated with *IL-1β* mRNA expression (*r* = 0.537, *P* = 0.012) and negatively correlated to PaO₂/Fio₂ ratios (*r* = 0.516, *P* = 0.017) in the cells from septic patients (fig. 1C), whereas *SphK2* mRNA expression correlated with neither *IL-1β* mRNA expression (*r* = 0.061, *P* = 0.794) nor PaO₂/Fio₂ ratios (*r* = 0.120, *P* = 0.605; Supplemental Digital Content, fig. S2, <http://links.lww.com/ALN/C272>). Taken together, these results suggest that *SphK1*, but not *SphK2*, plays an important role in sepsis.

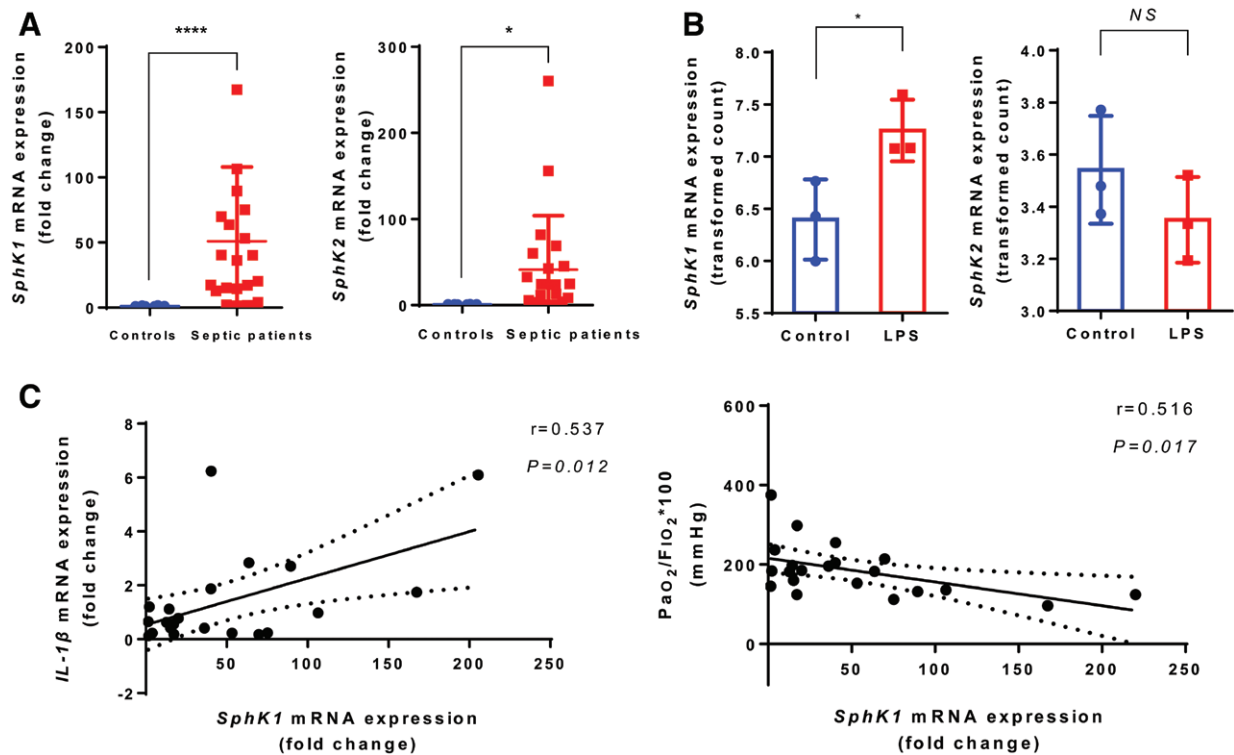


Fig. 1. *SphK1* messenger RNA (mRNA) expression correlates with interleukin (IL)-1 β mRNA expression and PaO₂/FiO₂ ratios in septic patients. (A) *SphK1* and *SphK2* mRNA expression in peripheral blood mononuclear cells of septic patients (n = 21) and healthy controls (n = 6) were assessed by real-time quantitative polymerase chain reaction. Dots represent data from individual subjects. Data are presented as means \pm SD with Mann-Whitney test. (B) *SphK1* and *SphK2* mRNA expression in health human monocytes treated with lipopolysaccharide (LPS; 100 ng/ml) for 4 h were downloaded from Gene Expression Omnibus for analysis (n = 3). Data are presented as means \pm SD with Student's two-tailed *t* test. (C) Correlation of *SphK1* mRNA expression with IL-1 β mRNA expression in peripheral blood mononuclear cells (left) and with PaO₂/FiO₂ (right) in septic patients (n = 21). Data were analyzed with linear regression analysis with a 95% confidence interval. **P* < 0.05, *****P* < 0.0001.

SphK1-Specific Inhibitor, PF-543, Improves Survivals and Attenuates Microvascular Leakage in Mice Polymicrobial Sepsis Model

To evaluate the roles of SphK1 in sepsis *in vivo*, we examined the effects of PF-543, a novel potent and specific inhibitor of SphK1, on survival and lung injury of septic mice. The 5-day mortality rate was 30% in PF-543-treated group and 80% in control group (N = 10 per group, *P* = 0.028; fig. 2A). Compared with mice in control group, mice in PF-543-treated group had better peripheral perfusion (fig. 2B), less microvascular permeability (Evan's blue dye index: 25.5 \pm 3.2 ng/g in control group *vs.* 18.2 \pm 1.4 ng/g in PF-543-treated group, *P* < 0.001), milder lung edema (wet/dry ratio: 8.0 \pm 0.2 in control group *vs.* 7.1 \pm 0.4 in PF-543-treated group, *P* < 0.0001), lower lung injury score (0.6 \pm 0.1 score/field in control group *vs.* 0.3 \pm 0.1 score/field in PF-543-treated group, *P* = 0.011), weaker myeloperoxidase activity in lung tissue (76.0 \pm 22.3 Δ OD460 nm \cdot min⁻¹ \cdot g⁻¹ in control group *vs.* 28.3 \pm 5.3 Δ OD460 nm

\cdot min⁻¹ \cdot g⁻¹ in PF-543-treated group, *P* < 0.001; fig. 2, C–F), and less inflammatory cell infiltration and tissue edema (Supplemental Digital Content, fig. S3, <http://links.lww.com/ALN/C272>). These results suggest that inhibition of SphK1 protects mice from sepsis-induced mortality and lung injury.

Specific-SphK1 Inhibitor, PF-543, Suppresses Interleukin-1 β Maturation and Release in Sepsis

To assess the effect of SphK1 on NLRP3 inflammasome activation, we first examined whether the specific SphK1 inhibitor, PF-543, could inhibit interleukin-1 β maturation and release. When lipopolysaccharide-primed macrophages were cotreated with PF-543 before adenosine triphosphate stimulation, interleukin-1 β maturation and release were suppressed by PF-543 in a dose-dependent manner (fig. 3A). In the experiments that followed, 1 μ M of PF-543 was chosen concerning the balance of effect and cytotoxicity. *In vivo*, interleukin-1 β concentration in serum and in

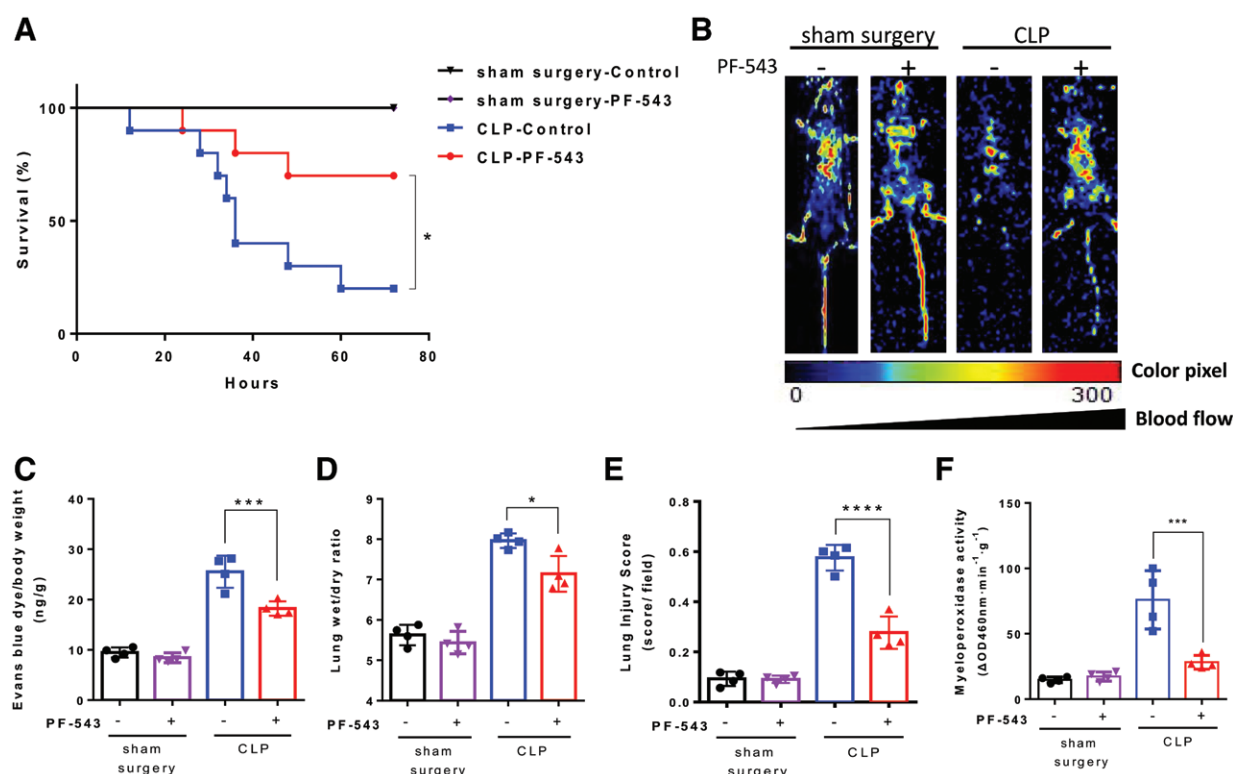


Fig. 2. Inhibition of sphingosine kinase 1 (SphK1) protects mice from sepsis-induced mortality and microvascular leakage. Mice were subjected to sham surgery or cecal ligation and puncture (CLP). Immediately after surgery, mice were intraperitoneally injected with PF-543 (10 mg/kg) or control. Mice were observed for 5 days after surgery. (A) Survival curves of each group are presented in Kaplan–Meier plots with log-rank (Mantel–Cox) test ($n = 10$ per group). (B) Peripheral perfusion was measured with laser Doppler imaging. Colored pixel (0–300) represents blood flow in region of interest from low to high. (C) Lung microvascular permeability was measured by Evan’s blue dye index. Data are presented as means \pm SD with one-way ANOVA, Tukey *post hoc* test. Dots represent data from individual mice ($n = 4$). (D) Wet/dry ratio was calculated to assess lung edema ($n = 4$). Data are presented as means \pm SD, with one-way ANOVA, Tukey *post hoc* test. Dots represent data from individual mice ($n = 4$). (E) Histologic lung injury was quantified according to lung injury score system. Dots represent data from individual mice ($n = 4$). Data are presented as means \pm SD, one-way ANOVA, Tukey *post hoc* test. (F) Neutrophil infiltration in the lung was assessed by lung tissue myeloperoxidase activity. Dots represent data from individual mice ($n = 4$). Scatter plots show means \pm SD, with one-way ANOVA, Tukey *post hoc* test. * $P < 0.05$; *** $P < 0.001$; **** $P < 0.0001$.

lung lysates of septic mice were lower in PF-543–treated group, compared with control group (fig. 3, B and C). In addition, activated caspase-1 in lungs of septic mice in PF-543–treated group was less than that in control group (fig. 3C). These results suggest that PF-543 inhibits interleukin-1 β maturation and release in macrophages, probably through suppressing caspase-1 activation.

SphK1 Mediates NLRP3 Inflammasome Activation in Sepsis

To address the role of SphK1 on NLRP3 inflammasome activation, we first tested the effect of PF-543 on *Casp-1*^{−/−} and *Nlrp3*^{−/−} macrophages. In accordance with previous reports, extracellular adenosine triphosphate–induced cleavage of pro–interleukin-1 β was dependent of caspase-1 and NLRP3 (fig. 4, A and B). Notably, PF-543 suppressed

adenosine triphosphate–induced caspase-1 activation and interleukin-1 β maturation in lipopolysaccharide–primed macrophages, which shared the same phenotype with *Casp-1* and *NLRP3* deletion (fig. 4, A and B). To explore the mechanism by which SphK1 influenced NLRP3 inflammasome activation, we performed coimmunoprecipitation in cell lysates. We found that PF-543 repressed the binding of ASC and pro–caspase-1 to NLRP3, and therefore prevented NLRP3 inflammasome complex assembly, and subsequent caspase-1 activation (fig. 4C). *In vivo*, no difference in the survival rates of *Nlrp3*^{−/−} septic mice was observed between PF-543–treated group and control group (fig. 4D). These results demonstrate that inhibition of SphK1 could block NLRP3 inflammasome activation.

To further confirm the effect of SphK1 on NLRP3 inflammasome activation, we examined whether genetic deletion of *SphK1* suppressed NLRP3 inflammasome

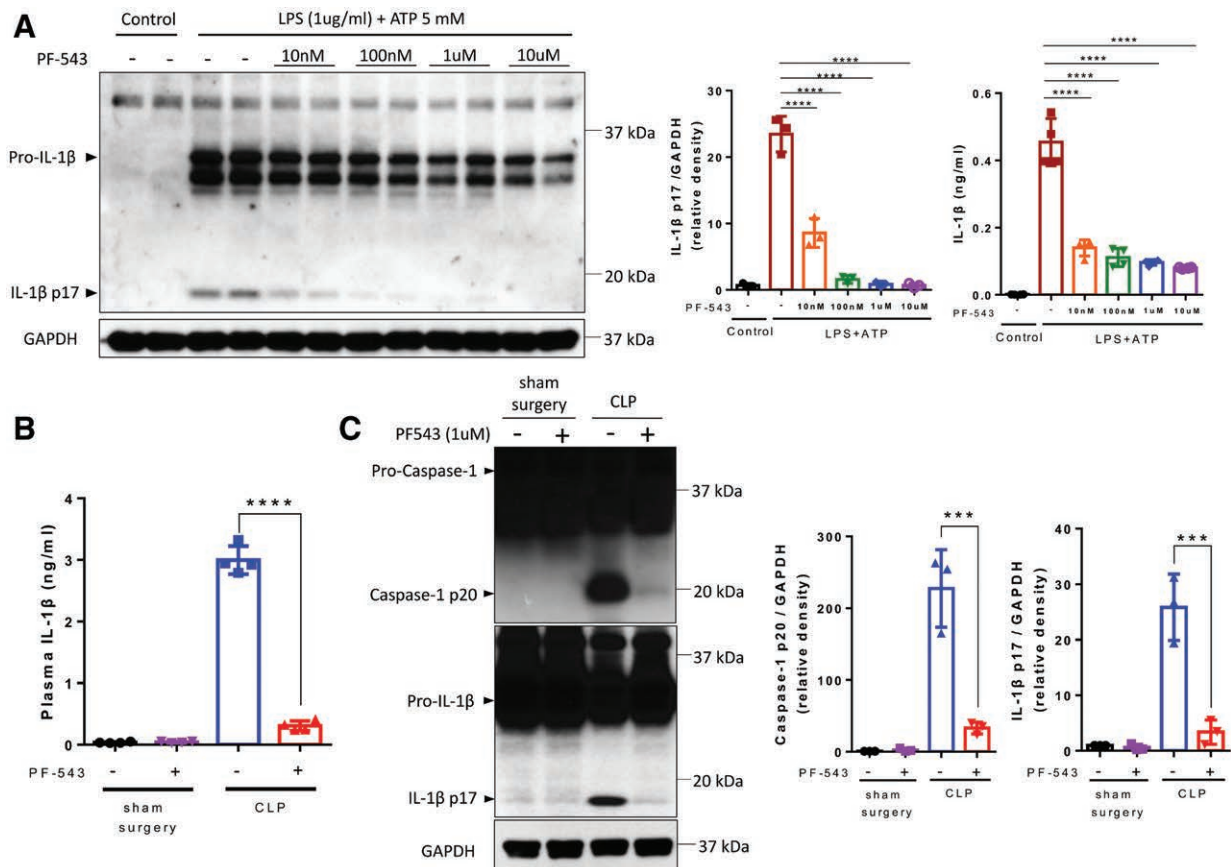


Fig. 3. Inhibition of sphingosine kinase 1 (SphK1) suppresses macrophage caspase-1 activation and reduces interleukin (IL)-1 β maturation and release. (A) Macrophages were primed with lipopolysaccharide (LPS; 1 μ g/ml) for 3 h, in combination with different doses of PF-543 as indicated or control, and subsequently incubated with adenosine triphosphate (ATP; 5 mM) for 30 min. Cell lysates were immunoblotted with IL-1 β antibody (left) and results are summarized in the middle panel ($n = 3$). IL-1 β release in supernatants was measured by enzyme linked immunosorbent assay (right, $n = 4$). (B and C) Mice were subjected to sham surgery or cecal ligation and puncture (CLP). Immediately after surgery, mice were intraperitoneally injected with PF-543 (10 mg/kg) or control. Lung tissues and serum were harvested from mice 24 h after surgery. IL-1 β in serum (B) was measured by enzyme-linked immunosorbent assay ($n = 4$). Lung lysates (C) were immunoblotted to assess caspase-1 activation and IL-1 β maturation ($n = 3$). (A–C) Data are shown as means \pm SD, with one-way ANOVA, Tukey *post hoc* test. *** $P < 0.001$; **** $P < 0.0001$.

activation. Consistent with the pharmacologic inhibition, genetic deletion of SphK1 blocked interleukin-1 β maturation and caspase-1 activation both *in vitro* and *in vivo* (Supplemental Digital Content, figs. S4 and S5, <http://links.lww.com/ALN/C272>). Compared with wild-type mice, *SphK1*^{-/-} mice had milder lung injury during sepsis (Supplemental Digital Content, fig. S6, <http://links.lww.com/ALN/C272>). These results suggest that SphK1 is required for NLRP3 inflammasome activation in sepsis.

Inhibition of SphK1 Protects Adherens Junction against Sepsis-induced Inflammation through Suppressing Interleukin-1 β Release

As is well illustrated, vascular endothelial cadherin plays a pivotal role in the maintenance of adherens junctions

and microvascular integrity. Phosphorylation of vascular endothelial cadherin by activated tyrosine-protein kinase Src results in vascular endothelial cadherin internalization and increase in vascular permeability.²⁴ To investigate the mechanism by which SphK1 protected septic mice from microvascular permeability, we measured vascular endothelial cadherin and Src activation in whole lung lysates. Compared with control group, Src phosphorylation and vascular endothelial cadherin degradation were reduced in PF-543-treated mice after cecal and ligation puncture (fig. 5A). Meanwhile, compared with control group, less interleukin-1 β deposited in lungs of septic mice in the PF-543-treated group (fig. 5B). To investigate whether interleukin-1 β impaired adherens junction in endothelium cells, we challenged endothelial monolayers with

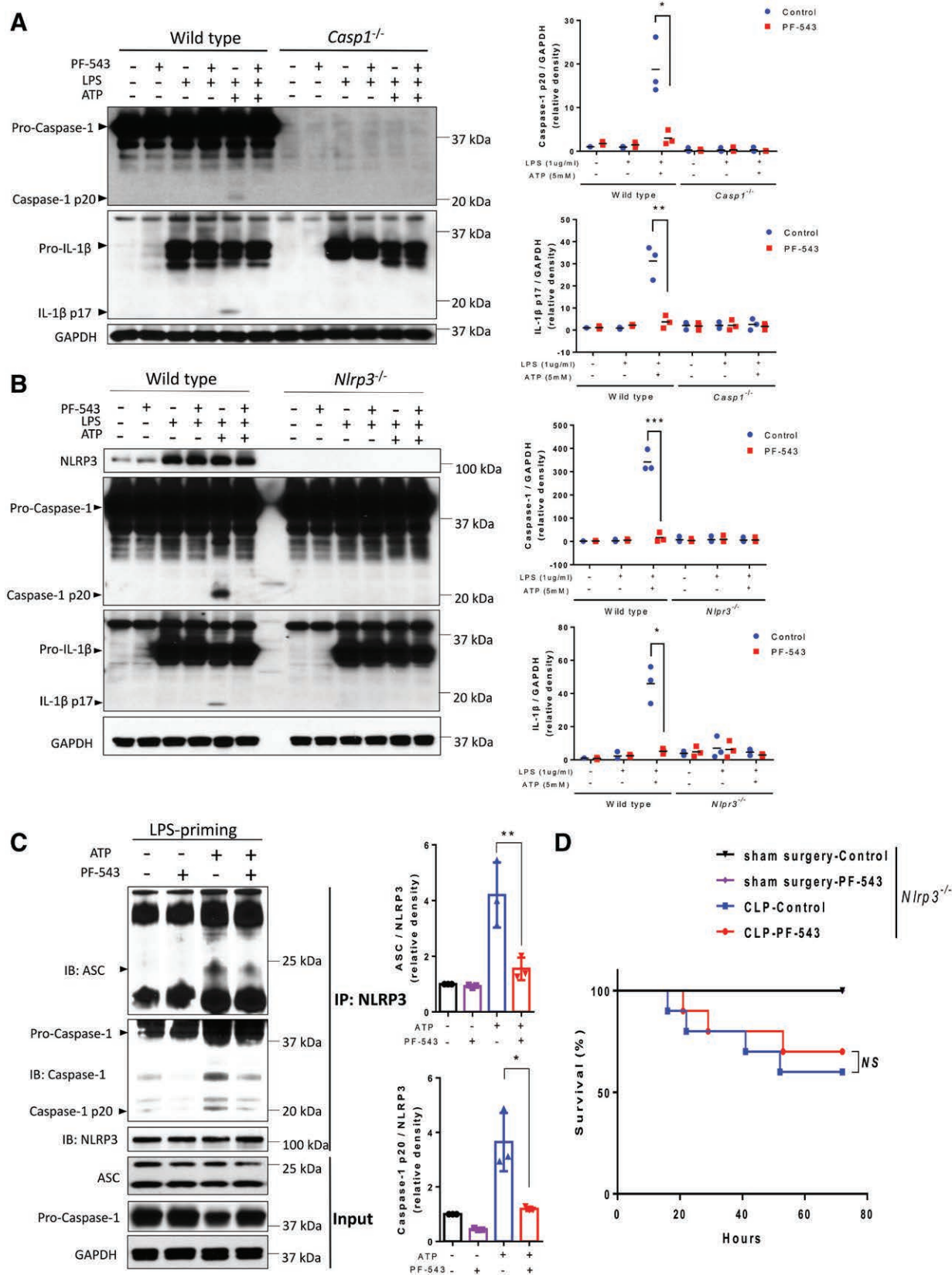


Fig. 4. (Continued)

Fig. 4. Inhibition of sphingosine kinase 1 (SphK1) suppresses nucleotide-binding oligomerization domain-like receptor containing pyrin domain 3 (NLRP3) inflammasome activation. (A and B) Macrophages were primed with lipopolysaccharide (LPS; 1 μ g/ml) for 3 h, in combination with PF-543 (1 μ M) or control, and subsequently incubated with adenosine triphosphate (ATP; 5 mM) for 30 min. Cell lysates were immunoblotted with antibodies as indicated (n = 3). Data are shown as means \pm SD, with Student's two-tailed *t* test. (C) Macrophage lysates were precipitated with anti-NLRP3 antibody, and immunoprecipitations were probed by immunoblot with anti-ASC antibody and anti-caspase-1 antibody (n = 3). Data are shown as means \pm SD, with one-way ANOVA, Tukey *post hoc* test. (D) *Nlpr3*^{-/-} mice were subjected to sham surgery or cecal ligation and puncture (CLP). Immediately after surgery, mice were intraperitoneally injected with PF-543 (10 mg/kg) or control (n = 10 per group). Survival curves of each group are presented in Kaplan–Meier plots with log-rank (Mantel–Cox) test. **P* < 0.05; ***P* < 0.01; ****P* < 0.001.

recombined human interleukin-1 β . Compared with control, interleukin-1 β stimulation resulted in increased endothelial permeability (fig. 5C), as well as enhanced Src activation and vascular endothelial cadherin phosphorylation (fig. 5D). Additionally, PF-543 alone did not influence Src activation and vascular endothelial cadherin phosphorylation in endothelial cells (Supplemental Digital Content, fig. S7, <http://links.lww.com/ALN/C272>). Furthermore, membrane vascular endothelial cadherin decreased (fig. 5E), whereas intracellular vascular endothelial cadherin increased in endothelial cells after interleukin-1 β stimulation (Supplemental Digital Content, fig. S8, <http://links.lww.com/ALN/C272>). Taken together, these results suggest that inhibition of SphK1 protects microvascular integrity from interleukin-1 β -mediated vascular endothelial cadherin internalization and adherens junction disassembly.

Discussion

Here we report that SphK1 in macrophages plays a proinflammatory role in sepsis. Selective inhibition of SphK1 protected mice from sepsis-induced mortality and lung injury. In mechanism, inhibition of SphK1 suppressed NLRP3/caspase-1-dependent interleukin-1 β activation and release from macrophages. Furthermore, we demonstrated that inhibition of SphK1 attenuated sepsis-induced microvascular leakage *via* suppressing interleukin-1 β -mediated vascular endothelial cadherin internalization and degradation (see Supplemental Digital Content, fig. S9, <http://links.lww.com/ALN/C272>, summarizing the mechanism by which inhibition of SphK1 suppresses vascular leakage in sepsis).

Sphingosine-1-phosphate is a biologically active signaling lipid which regulates diverse cellular processes.²⁵ Recent studies have demonstrated that sphingosine-1-phosphate plays a multifactorial role in innate immune cells maturation, activation, recruitment, and migration.²⁶ Sphingosine-1-phosphate is generated from sphingosine by two kinases, SphK1 and SphK2. Of the two kinase, SphK1 is the major kinase that catalyzed sphingosine-1-phosphate formation in blood. However, its role in sepsis remains controversial.^{27–31} We observed that *SphK1* and *SphK2* mRNA expression were both higher in septic patients, compared with healthy volunteers. Our analysis of *SphKs* mRNA expression from Gene Expression Omnibus database (fig. 1B) indicated that

lipopolysaccharide upregulated SphK1 mRNA expression, but not SphK2 mRNA expression, in human monocytes. To further confirm these observations, we recruited the second perspective cohort. We observed that *SphK1* mRNA expression, but not *SphK2* mRNA expression, was higher in peripheral blood mononuclear cells from septic patients in comparison with nonseptic patients. In addition, *SphK1* mRNA expression, but not SphK2 mRNA expression, in the cells positively correlated with interleukin-1 β mRNA expression and negatively correlated with PaO₂/Fio₂ ratios in septic patients. These human data suggest SphK1 is the major sphingosine kinase activated in monocytes during sepsis and may play a proinflammatory role.

Our *in vivo* results showed that inhibition of SphK1 suppressed lung injury in septic mice with promoted peripheral perfusion and alleviated microvascular leakage. *In vitro*, inhibition of SphK1 suppressed NLRP3 inflammasome activation and interleukin-1 β maturation in macrophages. All these results suggest that SphK1 in macrophages is profoundly involved in the pathogenesis of sepsis by upregulating innate immunity. On the contrary, Hla *et al.* have reported that SphK1 in macrophages is not essential for inflammatory response in sepsis.³¹ Compared with wild-type mice, *SphK1* knockout and *SphK1-SphK2* myeloid-specific double knockout mice exhibited no difference in survival and peritoneal macrophage recruitment when challenged with lipopolysaccharide and thioglycolate, respectively.³¹ However, there are some noticeable differences between this study and the study by Hla *et al.* Although peritoneal macrophage recruitment in a thioglycolate model was unchanged by loss of SphK1 and SphK2 in the study by Hla *et al.*, the thioglycolate model was used as a sterile peritonitis model, which is different from our cecal ligation and puncture-induced polymicrobial sepsis model. In the study by Hla *et al.*, a lethal dose of lipopolysaccharide (30 mg/kg intraperitoneally) was used to induce sepsis in mice, resulting in a very high mortality rate (more than 90%) in the wild-type group.³¹ Such a lethal dose of lipopolysaccharide may overwhelm the protective effect of SphK1 deletion. Even in such a lethal dose of lipopolysaccharide, *SphK1*^{-/-} mice presented a lower survival rate than wild-type mice by approximately 20%, reflecting a potential protective effect of *SphK1* deletion. Interestingly, protective effects of *SphK1* deletion were reported by Niessen *et al.*³²

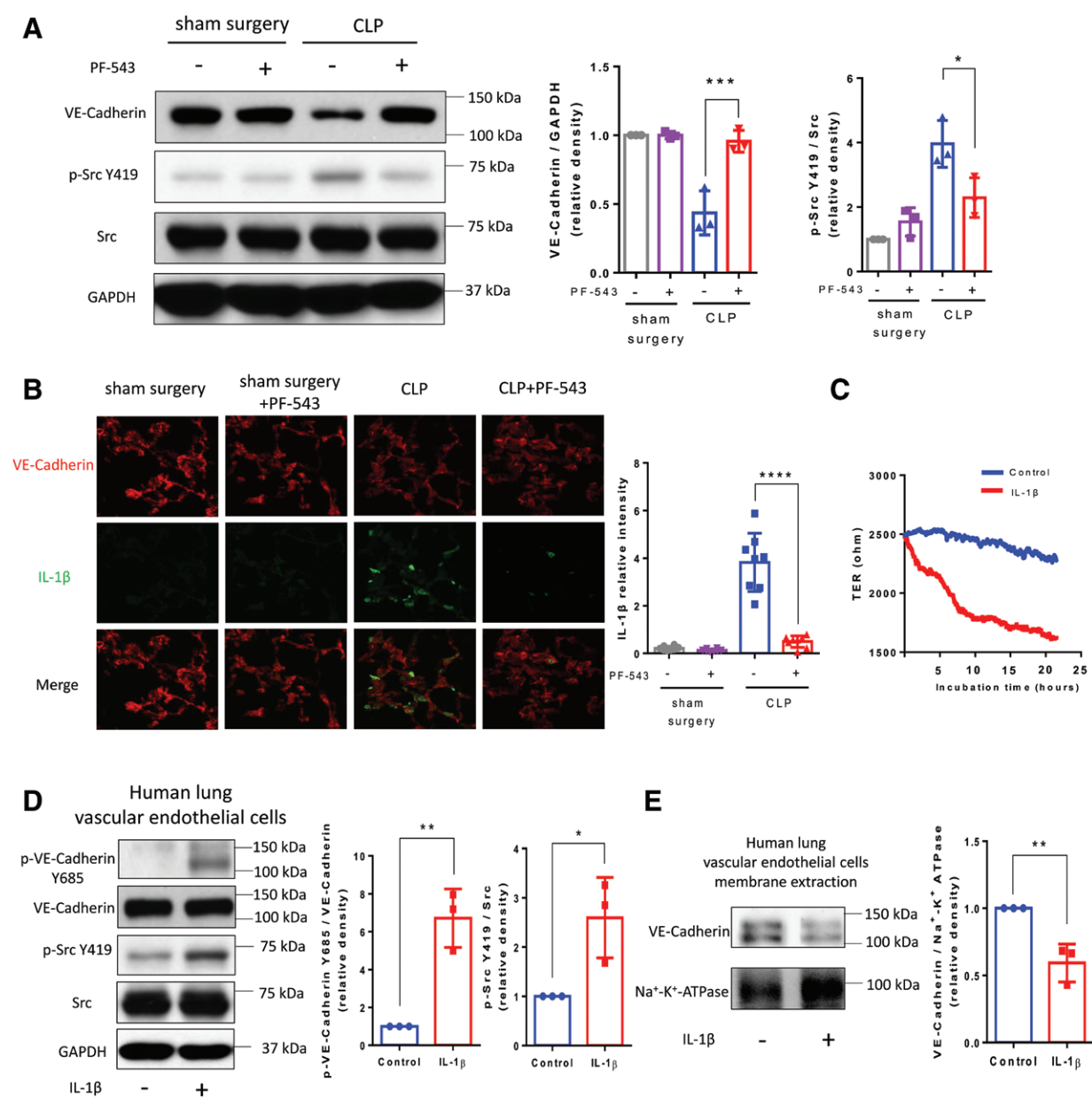


Fig. 5. Inhibition of sphingosine kinase 1 (SphK1) protects adherens junction integrity *via* suppressing interleukin (IL)-1 β release. (A) Lung tissues were harvested from mice 24 h after sham surgery or cecal ligation and puncture (CLP). Lung lysates were immunoblotted with indicated antibodies ($n = 3$). Data are shown as means \pm SD, with one-way ANOVA, Tukey *post hoc* test. (B) Representative immunofluorescence staining of lung sections ($n = 8$) from mice 24 h after surgery. Data are shown as means \pm SD, with one-way ANOVA, Tukey *post hoc* test. (C) Human lung microvascular endothelial monolayer treated with human recombinant IL-1 β (200ng/ml) or control. The integrity of endothelial cell monolayers was quantified by transendothelial electrical resistance assay. Data are shown as means \pm SD, with Student's two-tailed *t* test. (D and E) Endothelial cells were challenged with IL-1 β (200 ng/ml) for 24 h. Cell lysates (D) were immunoblotted with VE-cadherin, phosphorylated vascular endothelial (VE)-cadherin at Y685, Src and phosphorylated Src at Y419. Cell membrane extraction (E) was immunoblotted with VE-cadherin antibody. Data are shown as means \pm SD, with Student's two-tailed *t* test. * $P < 0.05$, ** $P < 0.01$; *** $P < 0.001$; **** $P < 0.0001$.

in mice challenged with 8 mg/kg lipopolysaccharide. In our sepsis model, the mortality rates were not so high as in the study by Hla *et al.*, with 80% in control group and 30% in

PF543-treated group, which revealed the protective effects of SphK1 inhibition covered up by the lethality in the study by Hla *et al.* Consistently, our experiments showed that

SphK1 deletion protected mice from sepsis-induced lung injury. Taken together, our data show that SphK1 promotes inflammatory responses and lung injury during polymicrobial sepsis.

NLRP3 inflammasomes are key components of host-defense system and triggers of inflammatory response to kill invading pathogens. However, excessive activation of the NLRP3 inflammasome pathway can also result in tissue injury and organ dysfunction. Pharmaceutical inhibition or genetic deletion of NLRP3 leads to a decline in serum interleukin-1 β concentration and prevents sepsis-induced organ failure, such as cardiac dysfunction, acute kidney injury, and muscle atrophy.^{33–35} Some insights imply the link between SphK1 and NLRP3 inflammasome activation in inflammation. Luheshi *et al.* reported that endogenous lipid sphingosine and its metabolite, sphingosine-1-phosphate, could induce NLRP3-inflammasome-dependent secretion of interleukin-1 β from macrophages.¹⁸ As reported in our results, adenosine triphosphate-induced interleukin-1 β maturation is dependent on NLRP3/caspase-1 and specific inhibition of SphK1 with PF-543 or *SphK1* deletion attenuated adenosine triphosphate-induced caspase-1 activation and interleukin-1 β release from macrophages. In line with *in vitro* results, inhibition of SphK1 did not alter the mortality of *Nlrp3*^{-/-} septic mice. These results suggest that SphK1 regulates NLRP3 inflammasome activation. Our work extends the findings of Luheshi *et al.* by identifying that SphK1, but not SphK2, is the key enzyme that regulates the NLRP3 inflammasome activation. Furthermore, we show that inhibition of SphK1 prevents assembly of NLRP3, ASC and caspase-1 to form inflammasome complex after challenging with extracellular adenosine triphosphate. Nonetheless, how SphK1 modulates the assembly of NLRP3 inflammasome needs to be further investigated.

In vascular endothelial cells, intercellular junctions maintain the vascular integrity. Both adherens junctions and tight junctions join neighboring cells together, and they adapt quickly to changes including inflammatory conditions.³⁶ The endothelial barrier is sealed by cell–cell adhesion molecules, among which vascular endothelial cadherin serves as a cornerstone.^{37,38} Vascular endothelial cadherin phosphorylation on tyrosine residue by nonreceptor tyrosine kinase Src has been shown to provoke its internalization both *in vitro* and *in vivo*, leading to adherens junction disassembly and increased vascular permeability,³⁹ resulting in microvascular leakage, which is considered as the central pathophysiologic change of sepsis.^{37,40} Our results show that Src activation and vascular endothelial cadherin internalization were significantly enhanced after interleukin-1 β stimulation in endothelial cells. *In vivo*, inhibition of SphK1 reduced deposition of interleukin-1 β in lungs. Meanwhile, it reversed Src phosphorylation and vascular endothelial cadherin degradation in lungs induced by sepsis. In addition, inhibition of SphK1 alone did not affect Src phosphorylation and vascular endothelial cadherin activation in

endothelial cells. These findings suggest that inhibition of SphK1 protects endothelium integrity by suppressing interleukin-1 β release from macrophages instead of its direct impact on endothelial cells.

In conclusion, we report that SphK1 plays a crucial role in NLRP3 inflammasome activation and contributes to lung injury and mortality in sepsis. Inhibition of SphK1 attenuates sepsis-induced inflammation and vascular leakage through suppression of NLRP3/caspase-1/interleukin-1 β pathway in macrophages. Furthermore, inhibition of SphK1 attenuates vascular leakage by suppressing interleukin-1 β -mediated vascular endothelial cadherin internalization and degradation in endothelial cells.

Acknowledgments

The authors thank Long Shuang Huang, Ph.D., and Zhigang Hong, Ph.D., Department of Pharmacology, University of Illinois, Chicago, Illinois, for their help in revising this manuscript.

Research Support

Support for this study was provided solely from institutional and/or departmental sources.

Competing Interests

The authors declare no competing interests.

Correspondence

Address correspondence to Dr. Zhu: Department of Critical Care Medicine, Zhongshan Hospital Fudan University, 180 Fenglin Road, Shanghai, China. zhuduming@fudan.edu.cn. Information on purchasing reprints may be found at www.anesthesiology.org or on the masthead page at the beginning of this issue. ANESTHESIOLOGY's articles are made freely accessible to all readers, for personal use only, 6 months from the cover date of the issue.

References

1. Singer M, Deutschman CS, Seymour CW, Shankar-Hari M, Annane D, Bauer M, Bellomo R, Bernard GR, Chiche JD, Cooper-Smith CM, Hotchkiss RS, Levy MM, Marshall JC, Martin GS, Opal SM, Rubenfeld GD, van der Poll T, Vincent JL, Angus DC: The third international consensus definitions for sepsis and septic shock (Sepsis-3). *JAMA* 2016; 315:801–10
2. Hotchkiss RS, Monneret G, Payen D: Sepsis-induced immunosuppression: From cellular dysfunctions to immunotherapy. *Nat Rev Immunol* 2013; 13:862–74
3. Mangan MSJ, Olhava EJ, Roush WR, Seidel HM, Glick GD, Latz E: Targeting the NLRP3 inflammasome in inflammatory diseases. *Nat Rev Drug Discov* 2018; 17:688

4. Yang Y, Wang H, Kouadir M, Song H, Shi F: Recent advances in the mechanisms of NLRP3 inflammasome activation and its inhibitors. *Cell Death Dis* 2019; 10:128
5. Grailer JJ, Canning BA, Kalbitz M, Haggadone MD, Dhond RM, Andjelkovic AV, Zetoune FS, Ward PA: Critical role for the NLRP3 inflammasome during acute lung injury. *J Immunol* 2014; 192:5974–83
6. Wu J, Yan Z, Schwartz DE, Yu J, Malik AB, Hu G: Activation of NLRP3 inflammasome in alveolar macrophages contributes to mechanical stretch-induced lung inflammation and injury. *J Immunol* 2013; 190:3590–9
7. Di A, Xiong S, Ye Z, Malireddi RKS, Kometani S, Zhong M, Mittal M, Hong Z, Kanneganti TD, Rehman J, Malik AB: The TWIK2 potassium efflux channel in macrophages mediates NLRP3 inflammasome-induced inflammation. *Immunity* 2018; 49:56–65.e4
8. Lee S, Nakahira K, Dalli J, Siempos II, Norris PC, Colas RA, Moon JS, Shinohara M, Hisata S, Howrylak JA, Suh GY, Ryter SW, Serhan CN, Choi AMK: NLRP3 Inflammasome deficiency protects against microbial sepsis via increased Lipoxin B4 synthesis. *Am J Respir Crit Care Med* 2017; 196: 713–26
9. Jin L, Batra S, Jeyaseelan S: Deletion of Nlrp3 augments survival during polymicrobial sepsis by decreasing autophagy and enhancing phagocytosis. *J Immunol* 2017; 198: 1253–62
10. Baker DA, Barth J, Chang R, Obeid LM, Gilkeson GS: Genetic sphingosine kinase 1 deficiency significantly decreases synovial inflammation and joint erosions in murine TNF- α -induced arthritis. *J Immunol* 2010; 185:2570–9
11. Lai WQ, Goh HH, Bao Z, Wong WS, Melendez AJ, Leung BP: The role of sphingosine kinase in a murine model of allergic asthma. *J Immunol* 2008; 180:4323–9
12. Snider AJ, Kawamori T, Bradshaw SG, Orr KA, Gilkeson GS, Hannun YA, Obeid LM: A role for sphingosine kinase 1 in dextran sulfate sodium-induced colitis. *FASEB J* 2009; 23:143–52
13. Tsai HC, Han MH: Sphingosine-1-phosphate (S1P) and S1P signaling pathway: Therapeutic targets in autoimmunity and inflammation. *Drugs* 2016; 76:1067–79
14. Maceyka M, Spiegel S: Sphingolipid metabolites in inflammatory disease. *Nature* 2014; 510:58–67
15. Tian T, Zhao Y, Huang Q, Li J: n-3 polyunsaturated fatty acids improve inflammation via inhibiting sphingosine kinase 1 in a rat model of parenteral nutrition and CLP-induced sepsis. *Lipids* 2016; 51:271–8
16. Zhang T, Yan T, Du J, Wang S, Yang H: Apigenin attenuates heart injury in lipopolysaccharide-induced endotoxemic model by suppressing sphingosine kinase 1/sphingosine 1-phosphate signaling pathway. *Chem Biol Interact* 2015; 233:46–55
17. Lufrano M, Jacob A, Zhou M, Wang P: Sphingosine kinase-1 mediates endotoxemia-induced hyperinflammation in aged animals. *Mol Med Rep* 2013; 8:645–9
18. Luheshi NM, Giles JA, Lopez-Castejon G, Brough D: Sphingosine regulates the NLRP3-inflammasome and IL-1 β release from macrophages. *Eur J Immunol* 2012; 42:716–25
19. Koch L, Linderkamp O, Ittrich C, Benner A, Poeschl J: Gene expression profiles of adult peripheral and cord blood mononuclear cells altered by lipopolysaccharide. *Neonatology* 2008; 93:87–100
20. Gong H, Rehman J, Tang H, Wary K, Mittal M, Chaturvedi P, Zhao YY, Komarova YA, Vogel SM, Malik AB: Corrigendum. HIF2 α signaling inhibits adherens junctional disruption in acute lung injury. *J Clin Invest* 2015; 125:1364
21. Matute-Bello G, Downey G, Moore BB, Groshong SD, Matthay MA, Slutsky AS, Kuebler WM; Acute Lung Injury in Animals Study Group: An official American Thoracic Society workshop report: Features and measurements of experimental acute lung injury in animals. *Am J Respir Cell Mol Biol* 2011; 44:725–38
22. Zhang X, Goncalves R, Mosser DM: The isolation and characterization of murine macrophages. *Curr Protoc Immunol* 2008; Chapter 14: Unit 14.1
23. Friedrich EE, Hong Z, Xiong S, Zhong M, Di A, Rehman J, Komarova YA, Malik AB: Endothelial cell Piezo1 mediates pressure-induced lung vascular hyperpermeability via disruption of adherens junctions. *Proc Natl Acad Sci USA* 2019; 116:12980–5
24. Gavard J: Endothelial permeability and VE-cadherin. *Cell Adh & Migr* 2014; 7: 465–71
25. Kunkel GT, Maceyka M, Milstien S, Spiegel S: Targeting the sphingosine-1-phosphate axis in cancer, inflammation and beyond. *Nat Rev Drug Discov* 2013; 12:688–702
26. Bryan AM, Del Poeta M: Sphingosine-1-phosphate receptors and innate immunity. *Cell Microbiol* 2018; 20:e12836
27. Bachmaier K, Guzman E, Kawamura T, Gao X, Malik AB: Sphingosine kinase 1 mediation of expression of the anaphylatoxin receptor C5L2 dampens the inflammatory response to endotoxin. *PLoS One* 2012; 7:e30742
28. Tauseef M, Kini V, Knezevic N, Brannan M, Ramchandaran R, Fyrst H, Saba J, Vogel SM, Malik AB, Mehta D: Activation of sphingosine kinase-1 reverses the increase in lung vascular permeability through sphingosine-1-phosphate receptor signaling in endothelial cells. *Circ Res* 2008; 103:1164–72
29. Kuchler L, Sha LK, Giegerich AK, Knape T, Angioni C, Ferreirós N, Schmidt MV, Weigert A, Brüne B, von Knethen A: Elevated intrathymic sphingosine-1-phosphate promotes thymus involution during sepsis. *Mol Immunol* 2017; 90:255–63

30. Michaud J, Kohno M, Proia RL, Hla T: Normal acute and chronic inflammatory responses in sphingosine kinase 1 knockout mice. *FEBS Lett* 2006; 580:4607–12
31. Xiong Y, Lee HJ, Mariko B, Lu YC, Dannenberg AJ, Haka AS, Maxfield FR, Camerer E, Proia RL, Hla T: Sphingosine kinases are not required for inflammatory responses in macrophages. *J Biol Chem* 2013; 288:32563–73
32. Niessen F, Schaffner F, Furlan-Freguia C, Pawlinski R, Bhattacharjee G, Chun J, Derian CK, Andrade-Gordon P, Rosen H, Ruf W: Dendritic cell PAR1-S1P3 signalling couples coagulation and inflammation. *Nature* 2008; 452:654–8
33. Huang N, Kny M, Riediger F, Busch K, Schmidt S, Luft FC, Slevogt H, Fielitz J: Deletion of Nlrp3 protects from inflammation-induced skeletal muscle atrophy. *Intensive Care Med Exp* 2017; 5:3
34. Arulkumaran N, Sixma ML, Pollen S, Ceravola E, Jentho E, Predecki M, Bass PS, Tam FWK, Unwin RJ, Singer M: P2X7 receptor antagonism ameliorates renal dysfunction in a rat model of sepsis. *Physiol Rep* 2018; 6
35. Wu D, Shi L, Li P, Ni X, Zhang J, Zhu Q, Qi Y, Wang B: Intermedin1–53 protects cardiac fibroblasts by inhibiting NLRP3 inflammasome activation during sepsis. *Inflammation* 2018; 41:505–14
36. Gavard J: Endothelial permeability and VE-cadherin: A wacky comradeship. *Cell Adh Migr* 2014; 8:158–64
37. Giannotta M, Trani M, Dejana E: VE-cadherin and endothelial adherens junctions: active guardians of vascular integrity. *Dev Cell* 2013; 26:441–54
38. Wallez Y, Huber P: Endothelial adherens and tight junctions in vascular homeostasis, inflammation and angiogenesis. *Biochim Biophys Acta* 2008; 1778:794–809
39. Benn A, Bredow C, Casanova I, Vukičević S, Knaus P: VE-cadherin facilitates BMP-induced endothelial cell permeability and signaling. *J Cell Sci* 2016; 129:206–18
40. Winkler MS, Nierhaus A, Poppe A, Greiwe G, Gräler MH, Daum G: Sphingosine-1-phosphate: A potential biomarker and therapeutic target for endothelial dysfunction and sepsis? *Shock* 2017; 47:666–72